

Washington University School of Medicine

Digital Commons@Becker

2020-Current year OA Pubs

Open Access Publications

11-16-2023

Contribution of macrophages to neural survival and intracochlear tissue remodeling responses following cochlear implantation

Muhammad Taifur Rahman
University of Iowa

Brian J Mostaert
University of Iowa

Bryce Hunger
University of Iowa

Utsow Saha
University of Iowa

Alexander D Claussen
University of Iowa

See next page for additional authors

Follow this and additional works at: https://digitalcommons.wustl.edu/oa_4

 Part of the [Medicine and Health Sciences Commons](#)

Please let us know how this document benefits you.

Recommended Citation

Rahman, Muhammad Taifur; Mostaert, Brian J; Hunger, Bryce; Saha, Utsow; Claussen, Alexander D; Razu, Ibrahim; Nasrin, Farjana; Khan, Nashwaan Ali; Eckard, Peter; Coleman, Sarah; Oleson, Jacob; Kirk, Jonathon R; Hirose, Keiko; and Hansen, Marlan R, "Contribution of macrophages to neural survival and intracochlear tissue remodeling responses following cochlear implantation." *Journal of neuroinflammation*. 20, 1. 266 (2023).
https://digitalcommons.wustl.edu/oa_4/3519

This Open Access Publication is brought to you for free and open access by the Open Access Publications at Digital Commons@Becker. It has been accepted for inclusion in 2020-Current year OA Pubs by an authorized administrator of Digital Commons@Becker. For more information, please contact vanam@wustl.edu.

Authors

Muhammad Taifur Rahman, Brian J Mostaert, Bryce Hunger, Utsow Saha, Alexander D Claussen, Ibrahim Razu, Farjana Nasrin, Nashwaan Ali Khan, Peter Eckard, Sarah Coleman, Jacob Oleson, Jonathon R Kirk, Keiko Hirose, and Marlan R Hansen

RESEARCH

Open Access



Contribution of macrophages to neural survival and intracochlear tissue remodeling responses following cochlear implantation

Muhammad Taifur Rahman¹, Brian J. Mostaert¹, Bryce Hunger¹, Utsow Saha¹, Alexander D. Claussen¹, Ibrahim Razu¹, Farjana Nasrin¹, Nashwaan Ali Khan¹, Peter Eckard¹, Sarah Coleman², Jacob Oleson², Jonathon R. Kirk³, Keiko Hirose⁴ and Marlan R. Hansen^{1*}

Abstract

Background Cochlear implants (CIs) restore hearing to deafened patients. The foreign body response (FBR) following cochlear implantation (post-CI) comprises an infiltration of macrophages, other immune and non-immune cells, and fibrosis into the scala tympani, a space that is normally devoid of cells. This FBR is associated with negative effects on CI outcomes including increased electrode impedances and loss of residual acoustic hearing. This study investigates the extent to which macrophage depletion by an orally administered CSF-1R specific kinase (c-FMS) inhibitor, PLX-5622, modulates the tissue response to CI and neural health.

Main text 10- to 12-week-old CX3CR1 +/GFP Thy1 +/YFP mice on C57BL/6J/B6 background was fed chow containing 1200 mg/kg PLX5622 or control chow for the duration of the study. 7 days after starting the diet, 3-channel cochlear implants were implanted in the ear via the round window. Serial impedance and neural response telemetry (NRT) measurements were acquired throughout the study. Electric stimulation began 7 days post-CI until 28 days post-CI for 5 h/day, 5 days/week, with programming guided by NRT and behavioral responses. Cochleae harvested at 10, 28 or 56 days post-CI were cryosectioned and labeled with an antibody against α -smooth muscle actin (α -SMA) to identify myofibroblasts and quantify the fibrotic response. Using IMARIS image analysis software, the outlines of scala tympani, Rosenthal canal, modiulus, and lateral wall for each turn were traced manually to measure region volume. The density of nuclei, CX3CR1 + macrophages, Thy1 + spiral ganglion neuron (SGN) numbers, and the ratio of the α -SMA + volume/scala tympani volume were calculated. Cochlear implantation in control diet subjects caused infiltration of cells, including macrophages, into the cochlea. Fibrosis was evident in the scala tympani adjacent to the electrode array. Mice fed PLX5622 chow showed reduced macrophage infiltration throughout the implanted cochleae across all time points. However, scala tympani fibrosis was not reduced relative to control diet subjects. Further, mice treated with PLX5622 showed increased electrode impedances compared to controls. Finally, treatment with PLX5622 decreased SGN survival in implanted and contralateral cochleae.

Conclusion The data suggest that macrophages play an important role in modulating the intracochlear tissue response following CI and neural survival.

Keywords Cochlear implant, Foreign body response, Fibrosis, Biomaterials, Inflammation

*Correspondence:

Marlan R. Hansen

marlan-hansen@uiowa.edu

Full list of author information is available at the end of the article



© The Author(s) 2023. **Open Access** This article is licensed under a Creative Commons Attribution 4.0 International License, which permits use, sharing, adaptation, distribution and reproduction in any medium or format, as long as you give appropriate credit to the original author(s) and the source, provide a link to the Creative Commons licence, and indicate if changes were made. The images or other third party material in this article are included in the article's Creative Commons licence, unless indicated otherwise in a credit line to the material. If material is not included in the article's Creative Commons licence and your intended use is not permitted by statutory regulation or exceeds the permitted use, you will need to obtain permission directly from the copyright holder. To view a copy of this licence, visit <http://creativecommons.org/licenses/by/4.0/>. The Creative Commons Public Domain Dedication waiver (<http://creativecommons.org/publicdomain/zero/1.0/>) applies to the data made available in this article, unless otherwise stated in a credit line to the data.

Introduction

Cochlear implants (CIs) provide auditory rehabilitation to individuals with moderate to severe sensorineural hearing loss. The device has undergone tremendous technological advancements to broaden the range of candidacy including those at the extremes of age, individuals with residual hearing or unilateral hearing loss, and patients with auditory neuropathy spectrum disorder [39]. Improved surgical techniques have led to a reduction in insertion trauma and electrode array translocation [16]. While modern surgical techniques and biocompatible implant materials enable a high rate of long-term device function, an intracochlear tissue response in the form of a foreign body response (FBR) or hypersensitivity reaction to the CI electrode array has been widely documented [29, 30, 32] primarily as a delayed phenomenon [13, 38]. This tissue response largely occurs within the scala tympani, a space that is normally devoid of cells making it unique to most other instances of FBR that occur in cellular tissues. Rahman et al. recently reviewed the current understanding of the inflammatory FBR following cochlear implantation, its impact on implant function in human subjects and animal models, and the emerging mitigation strategies for this deleterious response following cochlear implantation [38].

Histopathologic studies on human cochleae from CI recipients reveal an intrascalar tissue response that comprised densely organized fibrotic tissue and new bone growth [42] with variable severity occurring in a majority of cases [29]. This post-CI FBR is associated with significant detrimental consequences including loss of spiral ganglion neurons (SGNs), poorer auditory function [16], late-onset loss of residual low-frequency acoustic hearing [37], increased electrode impedances [44, 50], loss of acoustic hearing, poor word recognition scores, and, in rare cases, late-onset device failure [29]. While the FBR to electrode array biomaterials appears universal in human cochleae, it is exacerbated by traumatic insertion (e.g., electrode array translocation from scala tympani into scala vestibuli or media or damage to the lateral wall of the scala tympani).

Similar to humans, histological evidence for post-CI FBR occurs in animal models and is accompanied by loss of residual hearing, hair cells, and SGNs [38]. Hearing loss occurs early after implantation in guinea pigs and is followed by a partial recovery, which may be limited by the FBR [46, 55]. A correlation between fibrous tissue growth and sensory hair cell loss has been shown in cats [6], guinea pigs [33], and macaques [45]. Likewise, SGN loss is associated with electrode insertion trauma and inflammation in hearing cats [54]. The electrically evoked compound action potential (ECAP) reflects the synchronous response of auditory nerve fibers upon electrical

stimulation; ECAP amplitude growth function is used to assess the SGN population health. CI insertion trauma and the FBR appear to cause SGN dysfunction [36, 40] and, correspondingly, fibrosis and new bone formation are correlated with elevated ECAP thresholds in guinea pigs [47]. Further, a correlation between the extent of the FBR after cochlear implantation and electrical impedance changes has been documented in guinea pigs [52], kittens [31], cat [6, 54], and macaque models [45].

Macrophages have been identified in implanted human cochleae using antibodies to the markers CD163, Iba1, and CD68 [34]. These have been shown to phagocytize platinum and silicone from electrode arrays [30]. 'Activated' macrophages are present within the fibrotic sheath surrounding the electrode arrays [35] and demonstrate increased responses in cases of translocation of the electrode array and damage to the lateral wall [32]. In the mouse model, monocyte/macrophage (F4/80-positive cells) infiltrate in the cochlea in an apparent biphasic pattern: an early (3 days post-implantation) and late (14–28 days post-implantation) peaks [4, 7]. Macrophages can drive pro-inflammatory and pro-healing responses; their contribution to the unique FBR that develops within the cochlea remains unknown. Beyond cellular infiltration, a fibrotic tissue response develops within the scala tympani after CI, evident by the deposition of α -SMA-positive cells and type I collagen [4].

Given the deleterious consequences of the FBR, various strategies have been explored to mitigate this response. One such approach is the use of systemic or locally delivered glucocorticoids such as dexamethasone. Compared with standard CIs, electrode arrays that elute dexamethasone decrease fibrosis, bone growth, and electrical impedances, protect hair cells, and help preserve auditory function after implantation without affecting SGN density in guinea pigs [1, 3, 25, 47, 51, 52] and non-human primates [27]. Beyond dexamethasone, other anti-inflammatory medications that have been used to mitigate post-CI FBR include etanercept (a tumor necrosis factor-alpha receptor antagonist), lipoic acid, and others [38].

One limitation of these approaches is that they use nonspecific immunosuppressive agents that impact a variety of immune cell types and cytokines. While macrophages comprise a major immune cell type involved in FBR post-CI [7] other immune cell types including T and B lymphocytes, cytokines (CXCL1, IL-1 β , TNF- α) cell adhesion molecules (ICAM-1), connective tissue growth factor (CTGF), tissue remodeling proteins (TGF- β , MMP2, MMP9) are also involved in the FBR post-CI [38]. While non-selective anti-inflammatory drugs help mitigate the FBR post-CI and improve functional outcomes, these agents preclude the investigation of the contribution of specific cells or cytokines to the FBR.

In this study, we focused on determining the role of macrophages and the innate immune response to FBR post-CI and neural survival. To this end, we used the colony-stimulating factor 1 receptor (CSF-1R) inhibitor, PLX-5622, to deplete macrophages in a CX3CR1^{+/GFP} reporter mouse model of cochlear implantation. CSF1R is activated by 2 ligands, colony-stimulating factor-1 (CSF-1) and interleukin-34 (IL-34), and plays a critical role in the development of microglia and most tissue macrophages [49]. In selecting a CSF1R inhibitor, we considered several factors. First, the inhibitor needs to penetrate the blood–labyrinth barrier, and second, post-CI FBR is a chronic inflammatory condition where macrophages are involved for an extended period. Considering these factors, a highly selective CSF1R inhibitor, PLX5622 (PLX), that can cross the blood–brain barrier and allows extended elimination of macrophages was employed in this study [48].

Materials and methods

Animals

All the experimental protocols on mice in this study were approved by the University of Iowa Institutional Animal Care and Use Committee. For this study, we used both male and female 8- to 12-week-old CX3CR1^{+/GFP} Thy1^{+/YFP} mice ($n=29$) on a C57BL/6J/B6 background in which macrophages express GFP [18] and spiral ganglion neurons express YFP [11]. To maximize utilization of the available CX3CR1^{+/GFP} mice, some wildtype Thy1^{+/+} mice were used as well while no homozygous CX3CR1^{GFP/GFP} or Thy1^{YFP/YFP} subjects were used. Genotyping was performed for CX3CR1 and Thy1 using automated standard PCR of genomic DNA from tail samples, performed by Transnetyx genotyping services (<https://www.transnetyx.com/>).

PLX5622 administration

Macrophage depletion was achieved with the PLX5622 diet to determine the role of macrophages following cochlear implantation. Preliminary experiments on non-implanted mice were performed to confirm macrophage depletion with oral PLX5622 administration. Specifically, we fed 2 groups of CX3CR1^{+/GFP} Thy1^{+/YFP} mice with chow with PLX5622 (PLX) or control chow (No PLX). PLX-5622 compounds were formulated in AIN-76A standard chow by Research Diets Inc. at 1200 ppm as described previously. Based on results from previous studies, this dose is sufficient to deplete microglia in the brain within 7 days [9]. Therefore, we tested whether this dose (1200 ppm) and duration (7 days) is sufficient to eliminate cochlear macrophages. On day 7, all mice were euthanized for histopathologic examination and confocal

imaging. The timeline for this experiment is shown in Fig. 1a.

After confirmation of cochlear macrophage depletion with PLX5622 chow in nonimplanted mouse cochlear implantation on 2 groups of CX3CR1^{+/GFP} Thy1^{+/YFP} mice. In the PLX-5622 group (PLX), cochlear macrophages were depleted with oral administration of PLX5622 (1200 ppm for 7 days). In the ‘control’ (No PLX) group, CX3CR1^{+/GFP} Thy1^{+/YFP} mice were fed with ‘control chow’ for 7 days before CI surgery. On day 7, CI surgery was performed on both groups. Following recovery from surgery, mice from both groups were continued with respective chow (PLX or No PLX) until they were killed at 10, 28, and 56 days post-implantation. The timeline for this experiment is presented in Fig. 2a

Cochlear implantation

According to the previously described technique, CI surgery was performed on the left ears of mice (PLX or No PLX) through a round window approach with a custom 3 half-banded electrode cochlear implant (Cochlear Ltd., AUS) [7, 8].

Impedance measurement, neural response telemetry (NRT), and chronic electrical stimulation

Impedance measurements, NRT (8th nerve electrically evoked compound action potential), and programming for chronic electrical stimulation were performed in Custom Sound EP 4.2 (Cochlear Ltd., AUS) according to previously published protocol [8]. The Custom Sound programming software uses units of current level (CL) between 0 and 255, where 0 CL corresponds to 17.5 μ A and 0.44 nC/phase, and 255 CL corresponds to 1750 μ A and 43.75 nC/phase. Impedance measurements were performed for each separate electrode immediately before implantation. Immediately following surgery, impedance and NRT thresholds were measured and repeated at least weekly thereafter. Electrodes within compliance limits (defined as having electrical impedance ≤ 35 kOhms) were shorted together during electrical stimulation using a software patch. The hardware system for electrical stimulation consisted of a modified rodent housing with a sliding tether connected to a CI emulator (CIC4 implant emulator, Cochlear Ltd., AUS) which was activated by interfacing the receiver coil with a commercial CI sound processor (Cochlear Ltd., AUS). Starting on postoperative day 7, mice placed within and connected to the aforementioned system were stimulated for 5 h per day, 5 days a week, programmed to 30CL below the NRT threshold with a dynamic range of 1CL between threshold and comfort levels [8]. MAPs were reprogrammed weekly based on changes in electrode function and/or NRT threshold. Electrical stimulation was provided

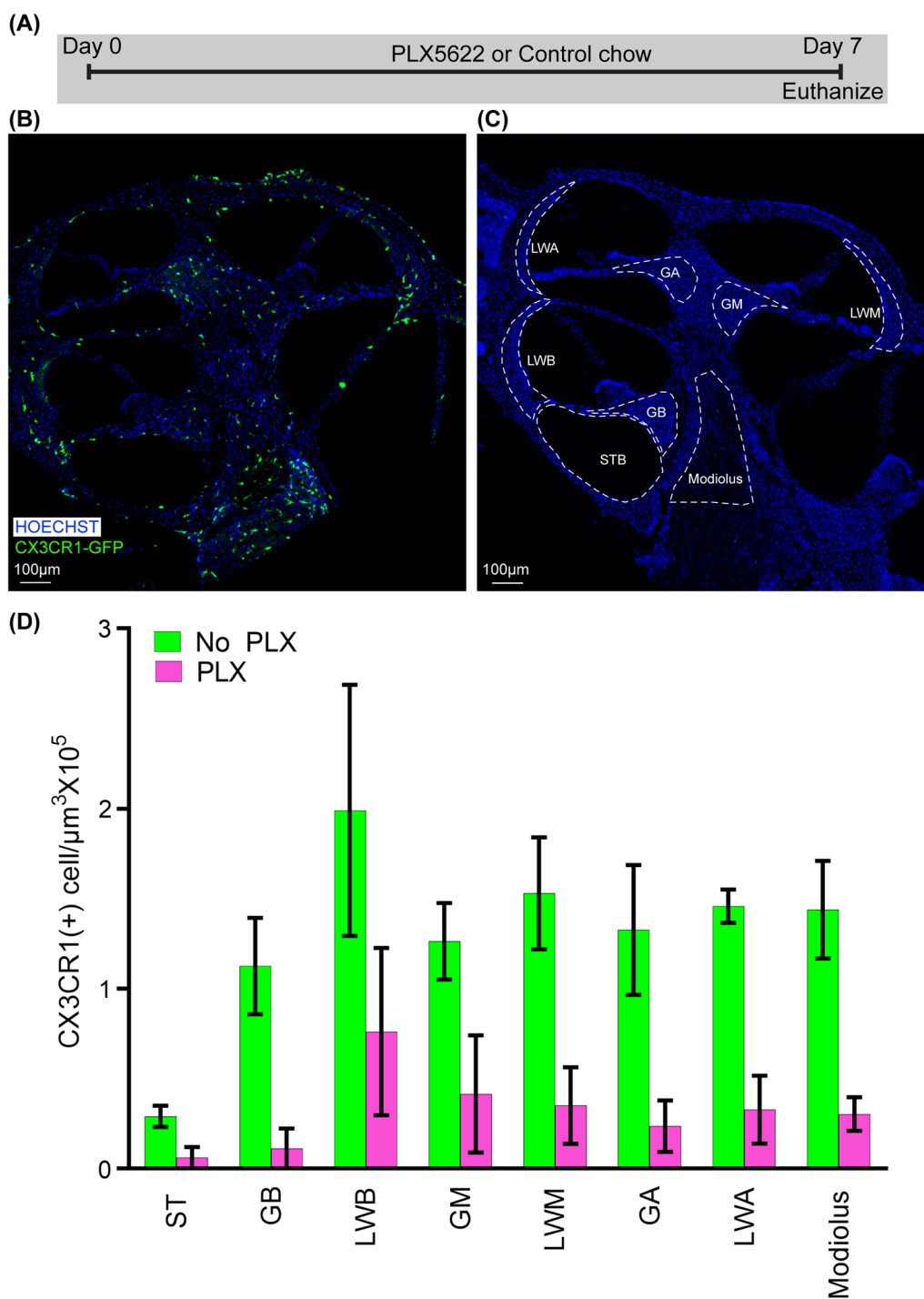


Fig. 1 Depletion of cochlear CX3CR1+ cells by oral administration of CSFR1 inhibitor, PLX5622. **A** Study design for oral administration of CSFR1 inhibitor, PLX5622. Two groups of 10- to 12-week-old CX3CR1^{+GFP} Thy1^{+YFP} mice with C57BL/6J/B6 background were fed chow mixed with PLX5622 (PLX) or control chow (No PLX). On day 7, all mice were euthanized, and labeled with Hoechst 3342 for histopathologic examination and confocal imaging. Confocal microscopy images showing CX3CR1-positive cells in **B** No-PLX (n=3) and **C** PLX (n=3) groups. **D** Graphical representation of the effect of 7 days of PLX-5622 treatment on cochlear resident CX3CR1-positive cells. ST: scala tympani of the base of the cochlea, GB: spiral ganglion of the basal turn of the cochlea, LWB: lateral wall of basal turn of the cochlea, GM: spiral ganglion of middle turn of cochlea, LWM: lateral wall of middle turn of cochlea, GA: spiral ganglion of apical turn of cochlea, LWA: lateral wall of middle turn of cochlea

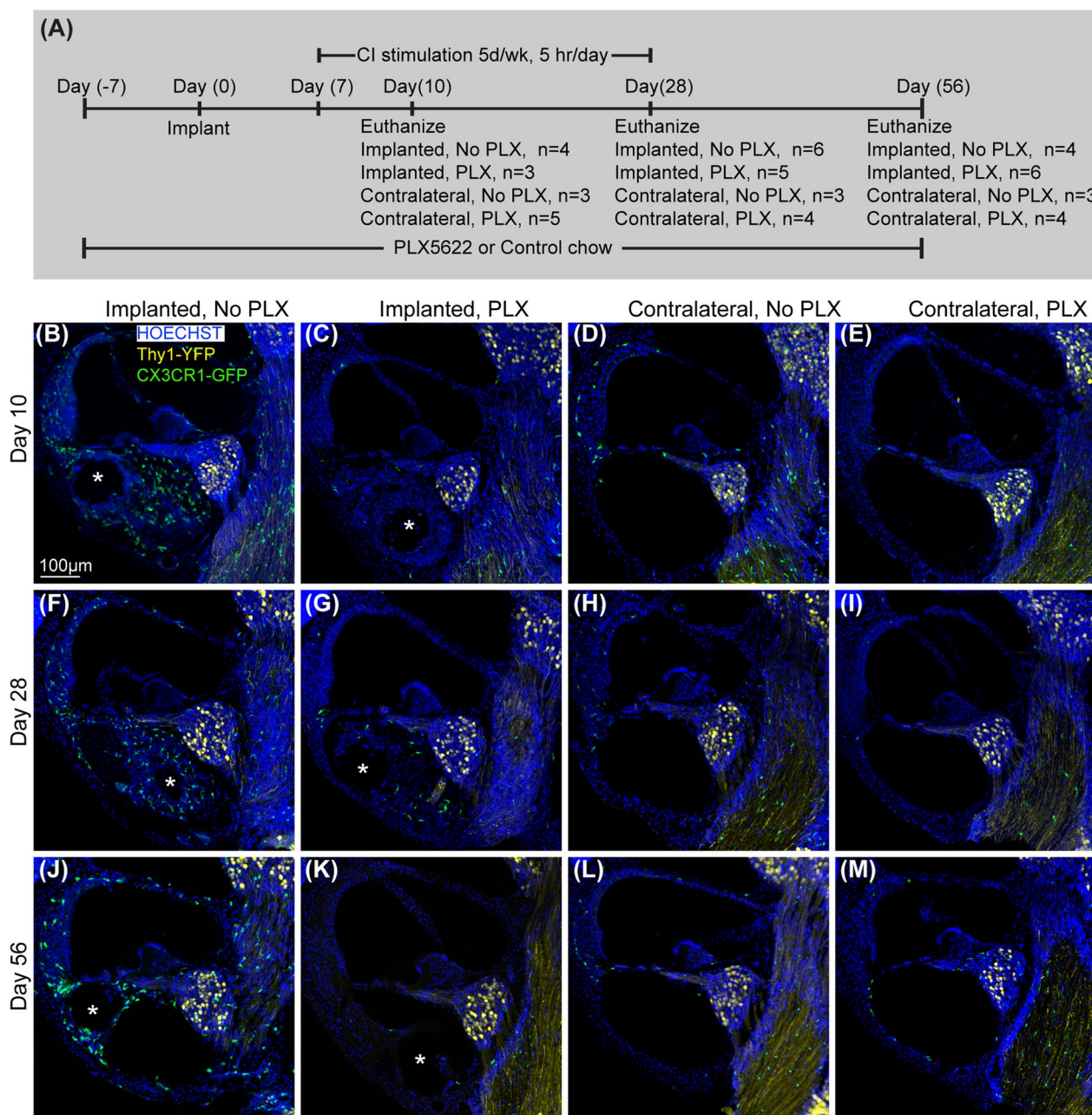


Fig. 2 Cochlear implantation following the elimination of cochlear macrophages. **A** Study design for cochlear implantation in PLX5662 treated mice. Cochlear implantation was performed on 2 groups of CX3CR1^{+/GFP} Thy1^{+/YFP} mice: one group was fed on chow with 1200 ppm of PLX-5622 (PLX) and the other group with control chow (No PLX) for 7 days. CI surgeries were performed on the left ear of both groups of mice after that (day 0). Following recovery from surgery, mice were continued with respective chow (PLX or No PLX) until they were killed at 10, 28, and 56 days post-implantation. Starting on post-operative day 7, mice within stimulation cages, connected to the CI processor were stimulated for 5 h per day, 5 days a week. **B–M** Fluorescent microscopic images of representative mid-modiolar, 30- μ m-thick sections of the basal turn of the cochlea from respective groups. The following labels were used (Hoechst, blue), macrophages (CX3CR1-GFP, green), and neurons, (Thy1-YFP, yellow). Asterisks indicate the tract of the CI. In the presence of a functional cochlear implant, macrophage (CX3CR1 + cells) infiltration into the cochlea appears to be sustained until the end of the study period (56 days post-CI). This was associated with the infiltration of other cells labeled with nuclear labeling Hoechst

through to 28 days postoperative. In this model and system electrode failures become more common beyond 28 days [8] and it becomes difficult to provide consistent stimulation across each group.

Immunohistochemistry

Under anesthesia with ketamine (80 mg/kg) and xylazine (10 mg/kg), mice were exsanguinated with transcatheter perfusion of ice-cold phosphate buffer solution (PBS) followed by transcatheter perfusion of 4% paraformaldehyde (PFA) at the final respective timepoint for each subject. Cochleae were harvested and were fixed overnight with 4% paraformaldehyde at 4 °C in the dark. Excess PFA was removed with PBS in a rotator overnight. Decalcification of cochlea was done in 0.1 M EDTA (pH 7.5) solution on a rotator that is changed every day for 3–5 days. After decalcification, cochlea washed with PBS 3 times, 10 min each time. Decalcified cochleae were cryoprotected using serial concentrations of sucrose solutions starting at 10% sucrose solutions and increasing concentration by 10% every hour, finally reaching 30%. Cryoprotected mice cochleae were stored at – 20 °C until sectioned. Cochlea infused with O.C.T. embedding medium (Tissue-TEK) were then mounted to the stage of sliding block microtome (American Optical 860) stage with O.C.T. and dry ice. Mounted cochleae were sectioned parallel to the mid-modiolar plane at 30 µm thickness, sections were placed on Fisher Superfrost slides, and stored at – 20 °C until immunolabeling was performed. For immunolabeling, slides were first warmed to room temperature (~20–22 °C), washed (3×5 min each wash) with ‘washing buffer’ containing TBS, 0.03% Triton X-100, and 0.1% Tween-20. Then samples were permeabilized and blocked in ‘blocking buffer’ (0.03% Triton X-100 and 0.1% Tween-20, 1% bovine serum albumin (RPI, CAS#9048-46-8) and 0.02% sodium azide (Sigma, catalog #S2002) in PBS) for 2 h. Following blocking, sections on slides were incubated in primary antibody (Alpha-smooth muscle actin monoclonal antibody, 1A4, eBioscience™, Catalog# 14-9760-82 at a dilution of 1000:1) in ‘blocking buffer’ overnight (~16 h) at 4 °C. After primary antibody application, sections were washed (3×5 min) in ‘washing buffer’, then incubated in blocking buffer containing secondary antibodies (Alexa Fluor™ 568, catalog# A-11004, Invitrogen, at a dilution of 1:400) for 2 h at room temperature. Sections were then washed 3×5 min in ‘washing buffer’. Nuclei were stained with Hoechst 3342 (10 µg/ml in PBS, Sigma) for 20 min at room temperature, followed by washing with ‘washing buffer’ (3×5 min) and coverslipped with Fluoro-Gel Mounting Medium with Tris Buffer (catalog #17985-10, Electron Microscopy Sciences).

Imaging and image analysis

For histological analysis of nuclei, macrophage, neurons, and fibrosis, 30-µm-thick sections from cochleae (implanted or contralateral) were immunolabeled, as described above, to visualize macrophage (CX3CR1-eGFP) neurons (Thy1-eYFP), nuclei (Hoechst 3342) and fibrotic tissue (anti-α-SMA antibody with Alexa 568 conjugated secondary antibody). Fluorescently labeled cochlear sections were imaged on a Leica Stellaris 5 confocal system using a 20 × (0.70 NA) objective, 0.75× digital zoom, z-axis-spacing of 1 µm, and constant exposure/gain settings throughout the experiment. Cochlear mid-modiolar sections were labeled for quantification of different cell types and tissues with the data from 3 adjacent sections averaged (“n” refers to the number of subjects). Image analysis was performed in IMARIS (Oxford Instruments, UK) image analysis software; cell counts, and quantitation of volumetric analyses were done on maximum intensity z-projections of 3D confocal image stacks. First, the outline of Rosenthal’s canal (RC) and the lateral wall in the basal, middle, and apical turns, the basal turn scala tympani, and modiolus were traced to measure the volume of each area. The number of macrophages (CX3CR1^{+/GFP}), neurons (Thy1^{+/YFP}), and nuclei (Hoechst 3342) were counted using an automated counting system in IMARIS image analysis software. The density of nuclei, macrophages, and neurons was calculated per 10⁵ µm³. Cell counting was restrained to the requirement of co-localizing nuclei (i.e., one neuron or macrophage counted per single co-localizing nuclei and reporter marker of interest). The fibrotic response was assessed by volumetric quantification of α-SMA in the basal scala tympani in mid-modiolar sections referenced to the volume of scala tympani. For histological analyses, we defined cochlear location by half-turn increments proceeding from the base to the apex, as previously described [21]. To allow quantitative comparison between experimental and control sections, image capture was performed using identical settings for imaging. Personnel performing cell counting, volumetric analyses, and other analyses were blind to the experimental conditions.

Statistical analyses

Statistical analyses for impedance measurements, counts of immune cells, nuclei, neurons, and volume of fibrotic tissue within scala tympani were performed using R version 4.3.0 (2023-04-21) (“R Core Team”, 2021). Specific comparisons that were made are described in respective figure legends. General linear models were fit to assess the main effects of group, day, and their interaction, except in impedance data where non-linear trends

were expected respective to time and a linear mixed model was fit. Shapiro–Wilk or D’Agostino–Pearson test was used to determine the normality of data. If model assumptions were not met, simpler models that excluded outlier groups were fit for parametric tests. For parametric data, pairwise comparisons of the least square means were made with Tukey adjustment for multiple comparisons. Additionally, non-parametric tests (e.g., Kruskal–Wallis test) were performed using Wilcoxon rank scores to compare all groups in data that were not normally distributed. Results of the statistical analysis are included in the text; as a regression analysis approach was used where comparisons are made on the regression models, no statistical annotations are included in the figures. Significance was defined as $p < 0.05$).

Results

PLX5622 depletes cochlear tissue-resident macrophages

Tissue-resident macrophages are a group of macrophages that are derived from the embryonic yolk sac and are independent of monocytes and bone marrow hematopoiesis [14]. Tissue-resident macrophages play a critical role in the initiation of inflammatory responses [10]. Therefore, we determined whether PLX5622 can deplete cochlear tissue-resident macrophages by treating CX3CR1^{+/GFP} reporter mice with PLX5622 (PLX). Figure 1 presents representative mid-modiolar sections of cochleae from CX3CR1^{+/GFP} reporter mice following 7 days of administration of PLX5622 (PLX) or control chow (No PLX). In cochleae from No PLX mice, CX3CR1-positive cells exist in specific regions: scala tympani of the base of the cochlea, spiral ganglion, modiolus, and lateral wall (base, middle, and apex). Seven days of oral treatment with chow containing 1200 ppm of PLX-5622 nearly eliminates (~80%) these resident CX3CR1-positive macrophages (unpaired t-test, $p = 0.0001$). Going forward we used this protocol to deplete resident macrophages before cochlear implantation.

PLX5622 reduces macrophage infiltration post-CI

Unlike tissue-resident macrophages, infiltrating or inflammatory macrophages are thought to be derived from circulating monocytes, and are often called monocyte-derived or bone marrow-derived macrophages [23]. We next examined whether PLX5622 also reduces the CX3CR1-positive cochlear macrophage population following cochlear implantation. After 7 days of treatment with either PLX-5622 chow (PLX) or control chow (No PLX), left cochleae of CX3CR1^{GFP/+} Thy1^{YFP/+} mice were implanted and stimulated for up to 28 days post-CI while right cochleae served as unimplanted controls. Animals were euthanized at 10, 28, or 56 days post-CI. Representative mid-modiolar sections across groups and time points are seen in Fig. 2. Figure 3 demonstrates the quantification of CX3CR1-positive cell density in different regions of cochlea across the study period. In the No PLX unimplanted cochleae, CX3CR1+ cells were dispersed throughout the cochlea including a very low density along the margin of the scala tympani of the base. These cells demonstrate the classical ramified morphology of tissue macrophages. Compared to the contralateral side, No PLX-implanted cochleae showed significant infiltration of CX3CR1-positive cells throughout the cochlea (Figs. 2 and 3). While most of the infiltrating CX3CR1+ cells exhibited a ramified morphology in the No PLX-implanted cochleae, a small subset of amoeboid CX3CR1-positive cells were observed in the scala tympani. A major influx of CX3CR1-positive cells within the modiolus, the scala tympani, spiral ganglion, lateral wall of the base middle, and apical turn was observed following implantation in No PLX (Kruskal–Wallis test on Wilcoxon rank scores, $p < 0.0001$ comparing all groups, a parametric model could not be fit to include No PLX implanted) as shown in Fig. 3. Within the specified period (10 through 56 days post-CI), time following cochlear implantation does not significantly affect the density of CX3CR1-positive cells (no effect of day in

(See figure on next page.)

Fig. 3 Quantification of CX3CR1 + macrophage density in the cochlea following cochlear implantation. Cochlear implantation was performed in CX3CR1^{+/GFP} Thy1^{+/YFP} mice, fed on chow with 1200 ppm of PLX-5622 (PLX) or control chow (No PLX) for 7 days. Following surgery, mice were continued with respective chow (PLX or No PLX). Starting on post-operative day 7, mice within stimulation cages, connected to the CI processor were stimulated for 5 h per day, 5 days a week. Mice were euthanized at 10, 28 and 56 days post-CI and imaged. Image analysis was performed in IMARIS image analysis software. In 30- μm -thick mid-modiolar sections, CX3CR1 + macrophage cells were counted on maximum intensity z-projections of 3D confocal image stacks. The outline of Rosenthal’s canal (RC) and lateral wall at the base, middle, and apex of the cochlea, scala tympani of the base of the cochlea, and modiolus was traced and the volume of each area was measured. CX3CR1 + macrophages were counted using an automated counting system in IMARIS image analysis software aided by custom-made macros. The density of macrophages with visible, Hoechst + nuclei was calculated per $10^5 \mu\text{m}^3$ in each area mentioned. Values derived from every region of the cochlea for an individual animal were averaged together from 3 sections; “n” is the total number of mice used in the study. **A–H** Density of macrophage in different locations of cochlea in different treatment groups. Number of cochlea analyzed in this study are as follows: at day 10 post-CI, implanted ‘no PLX’ ($n = 4$), implanted PLX, ($n = 3$), contralateral ‘no PLX’ ($n = 3$), contralateral PLX ($n = 5$); at day 28 post-CI, implanted ‘no PLX’ ($n = 6$), implanted PLX, ($n = 5$), contralateral ‘no PLX’ ($n = 3$), contralateral PLX ($n = 4$); at day 56 post-CI, implanted ‘no PLX’ ($n = 3$), implanted PLX, ($n = 6$), contralateral ‘no PLX’ ($n = 3$), contralateral PLX ($n = 4$). Error bars indicate SEM

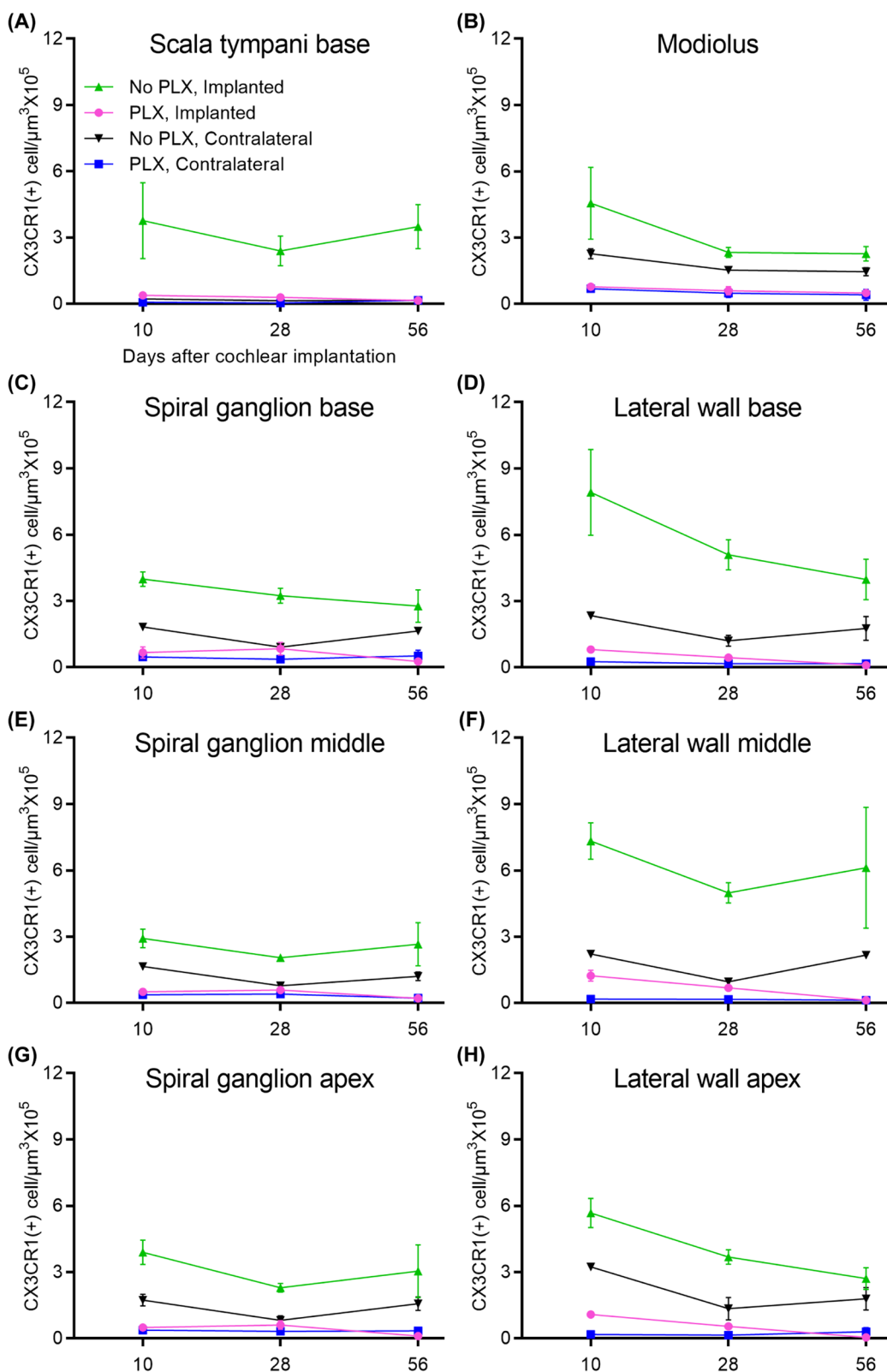


Fig. 3 (See legend on previous page.)

general linear model in all cases, $p > 0.05$) except in the lateral wall of the base, where a main effect of the day was seen ($p = 0.0013$) with pairwise comparisons on the least squares means with Tukey adjustment showing day 10 macrophage density was significantly different from day 28 ($p = 0.0016$) and 56 ($p = 0.0096$), with no difference between day 28 and 56 ($p = 0.7202$) (Fig. 3).

Orally administered PLX5622 effectively reduced the resident macrophage population throughout the cochlea for the study duration in unimplanted cochleae compared to No PLX (pairwise comparisons of No PLX and PLX unimplanted groups on least squares mean effect of the group using Tukey adjustment, $p < 0.05$ in all areas except scala tympani of the base, $p = 0.4295$, where little to no macrophage infiltration was seen in either group). Likewise, oral administration of PLX5622 reduced the infiltration of CX3CR1-positive cells throughout implanted cochlea at all time points compared to No PLX implanted (Kruskal–Wallis test on Wilcoxon rank scores of non-parametric data, $p < 0.0001$ in all cases, a parametric model could not be fit to include No PLX implanted) (Fig. 3).

PLX5622 treatment does not reduce cellular density within cochlea post-CI

Cochlear implantation resulted in an increased density of Hoechst+ cells in the cochlea in PLX and No PLX groups relative to unimplanted groups, shown histologically in Fig. 2 and quantified in Fig. 4 and Supplementary Fig. 1. The time following cochlear implantation (10 through 56-day post-CI) does not significantly affect cellular density (no effect of day in the parametric model including No PLX and PLX implanted groups, $p = 0.8304$). A trend of reduced cellular density was seen in the PLX implanted compared to the No PLX implanted approached, but this did not reach statistical significance (no effect of group in the parametric model including No PLX and PLX implanted groups, $p = 0.0829$). As the data were not normally distributed, we used additional non-parametric testing on Wilcoxon rank scores to assess all 4 groups. The Kruskal–Wallis test was significant $p < 0.0001$, suggesting a difference between groups in scala tympani nucleus density in the basal turn (Figs. 2 and 4).

PLX5622 does not affect fibrosis post-CI

Following cochlear implantation in PLX and No PLX mice, α -SMA+ fibrotic tissue grows into the scala tympani of the base of the cochlea adjacent to the electrode array (Fig. 5). Fibrosis is seen at 10 days post-CI and is maintained throughout the 56-day post-CI timepoint and time following cochlear implantation (10 through 56 days post-CI) does not significantly affect the volume of the fibrotic response (no effect of day in the parametric

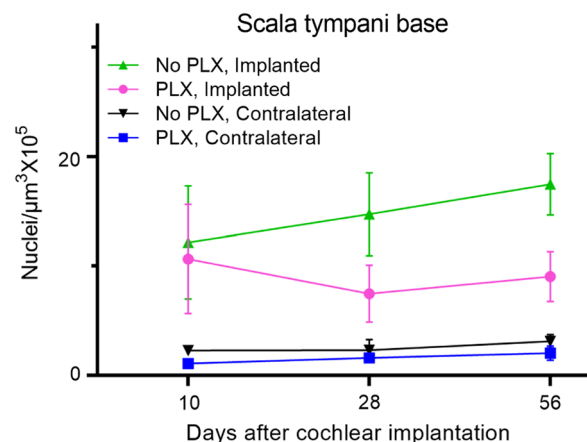


Fig. 4 Quantification of cellular density into scala tympani of the base of cochlea following cochlear implantation. Cochlear implantation was performed in CX3CR1^{+/GFP} Thy1^{+/YFP} mice, fed on chow with 1200 ppm of PLX-5622 (PLX) or control chow (No PLX) for 7 days. Treatment with respective diets and electrical stimulation was continued until the desired endpoints (10, 28, or 56 days). Nuclei were labeled with Hoechst 3342 in 30-μm-thick mid-modiolar sections. Image analysis was performed in IMARIS image analysis software. Hoechst+ cells were counted on maximum intensity z-projections of 3D confocal image stacks in scala tympani of the base of the cochlea. The volume of scala tympani and nuclear counts were made using an automated counting system in IMARIS image analysis software aided by custom-made macros. Nuclear density (Hoechst+ cells) was calculated per $10^5 \mu\text{m}^3$. An average of 3 sections per animal was taken with 'n' being the number of animals. Number of cochlea analyzed in this study are as follows: at day 10 post-CI, Implanted 'no PLX' ($n = 4$), implanted PLX, ($n = 3$), contralateral 'no PLX' ($n = 3$), contralateral PLX ($n = 5$); at day 28 post-CI, Implanted 'no PLX' ($n = 6$), implanted PLX, ($n = 5$), contralateral 'no PLX' ($n = 3$), contralateral PLX ($n = 4$); at day 56 post-CI, Implanted 'no PLX' ($n = 3$), implanted PLX, ($n = 6$), contralateral 'no PLX' ($n = 3$), contralateral PLX ($n = 4$). Error bars indicate SEM

model including PLX and No PLX implanted groups, $p = 0.5975$). Unlike the macrophage and cellular infiltration, the volume of α -SMA+ fibrotic tissue in basal turn was not affected by PLX5622 treatment (no effect of group in the parametric model including PLX and No PLX implanted groups, $p = 0.5975$) (Fig. 5).

PLX5622 increases electrode impedance

Figure 6 shows mean electrode impedance values for No PLX and PLX groups over time for active electrodes (i.e., electrodes with an open circuit denoting hardware failure were excluded). The trends in impedance growth over time for PLX and No PLX groups appeared non-linear, thus we used a linear mixed model using the square root of days. The PLX and No PLX groups showed similar baseline electrode impedance values at peri-operative baseline testing (linear mixed model, day 0 y-intercept, $p = 0.9341$). Both PLX (slope = 8.47 kOhm/square root of days $p < 0.0001$) and No PLX (slope = 4.05 kOhm/

square root of days $p=0.0018$) showed statistically significant increases in impedance over time, with the rate of increase in the PLX group being greater (group \times square root of day interaction, $p=0.0067$). We used contrasts (Kenward–Roger degrees of freedom and a Bonferroni alpha level correction) from the linear mixed model to assess at what point the two groups diverged in impedance growth over time. We observed that the PLX impedance values began to significantly differ from the No-PLX between day 14 and 21 and persisted up to day 56. ($p=0.06$ and 0.02 at 14 and 21 days post-CI, respectively; Kenward–Roger degrees of freedom and Bonferroni alpha level correction). Day 21 post-CI and onward, electrical impedance in the PLX group was consistently higher compared to the No PLX group ($p=0.0056$ – 0.0104 ; Kenward–Roger degrees of freedom and Bonferroni alpha level correction).

PLX5622 causes SGN degeneration

Figure 7 shows the mean density of Thy1^{YFP} + SGNs for the ‘No PLX’ and ‘PLX’ groups over time. First, we considered the change in SGN density over time in the base (significant effect of day in a parametric model, $p<0.0001$). In the spiral ganglion of the base of the cochlea, SGN density at day 28 is significantly lower than that of day 10 (pairwise comparison on least squares means for the effect of the day with Tukey adjustment, $p<0.0001$). The difference between day 10 and 56 was also significant (pairwise comparison on least squares means for the effect of the day with Tukey adjustment, $p=0.0011$). The difference between day 28 and day 56 was non-significant. Similarly, SGN degeneration is observed in the middle turn of the cochlea from day 10 to day 28 (significant effect of day in a parametric model, $p=0.0004$; pairwise comparison on least squares means for the effect of the day with Tukey adjustment, $p=0.0003$). In the apical turn, density at day 28 is significantly lower from day 10 (significant effect of day in a parametric model, $p=0.0120$; pairwise comparison on least squares means for the effect of day with Tukey adjustment, $p=0.0148$) The difference between day 10

and day 56 in apical neuron density was marginally significant ($p=0.0503$), but the difference between day 28 and day 56 was non-significant ($p=0.96$). These experiments are done on mice with a B6 background and suggest that significant SGN degeneration happens in these mice between 3 and 4 months of age. Next, we considered the effect of cochlear implantation on SGN density. Following cochlear implantation, we did not observe evidence for SGN degeneration in cochleae compared to respective PLX and No PLX unimplanted groups (significant effect of group in the parametric model of apical, middle, and basal neuron density, $p=0.0001$ – 0.0051 ; pairwise comparison on least squares means for the effect of days with Tukey adjustment, $p>0.05$).

We also considered whether PLX treatment causes degeneration of SGNs in unimplanted condition. Compared to No PLX mice, in PLX mice, SGN density was significantly lower in the contralateral (unimplanted) cochlea at the basal turn ($p=0.0053$), middle turn ($p=0.0002$) and apical turn ($p=0.0148$) (significant effect of group in the parametric model of apical, middle and basal neuron density, $p=0.0001$ – 0.0051 ; pairwise comparison on least squares means for the effect of days with Tukey adjustment). We further analyzed the impact of PLX treatment on the implanted cochlea. In the implanted cochlea, PLX treatment is associated with SGN degeneration in the base only ($p<0.0001$ significant effect of group in parametric model apical, middle and basal neuron density, $p=0.0001$ – 0.0051 ; pairwise comparison on least squares means for the effect of days with Tukey adjustment). After looking at pairwise comparisons in the group \times day interaction, we found that the only significant differences between treatment groups are in days 10 and 28. On day 10 post-CI, the mean for PLX-CI is significantly lower than no-PLX CI ($p=0.0202$), and on day 28, PLX CI is significantly lower than No PLX CI ($p=0.0487$); pairwise comparison on least squares means for day \times group interaction with Tukey adjustment. Thus, PLX5622 administration was associated with SGN degeneration irrespective of cochlear implantation status.

(See figure on next page.)

Fig. 5 Quantification of α -SMA + tissue within scala tympani of the base of the cochlea following cochlear implantation. Following 7-day feeding on chow with 1200 ppm of PLX-5622 (PLX) or control chow (No PLX), cochlear implantation was performed in $\text{CX3CR1}^{+/GFP} \text{Thy1}^{+/YFP}$ mice. Respective diets were resumed following recovery from surgery. Electrical stimulation was continued until 28 days post-CI. Mice were euthanized at the desired endpoints (10, 28, or 56 days). Following euthanasia, 30 μm mid-modiolar sections were labeled with anti- α -SMA antibodies. **A–L** Representative images are shown. Asterisks within the images indicate the tract of the CI, **M** analyses the data. The volume of the scala tympani and α -SMA + tissue volumes were measured using IMARIS image analysis software. Fibrosis was measured by dividing the volume of α -SMA + tissue by the volume of scala tympani, expressed in % volume. Number of cochlea used in this study are as follows: at day 10 post-CI, implanted ‘no PLX’ ($n=4$), implanted PLX, ($n=3$), contralateral ‘no PLX’ ($n=3$), contralateral PLX ($n=5$); at day 28 post-CI, Implanted ‘no PLX’ ($n=6$), implanted PLX, ($n=5$), contralateral ‘no PLX’ ($n=3$), contralateral PLX ($n=4$); at day 56 post-CI, implanted ‘no PLX’ ($n=3$), implanted PLX, ($n=6$), contralateral ‘no PLX’ ($n=3$), contralateral PLX ($n=4$). Error bars indicate SEM

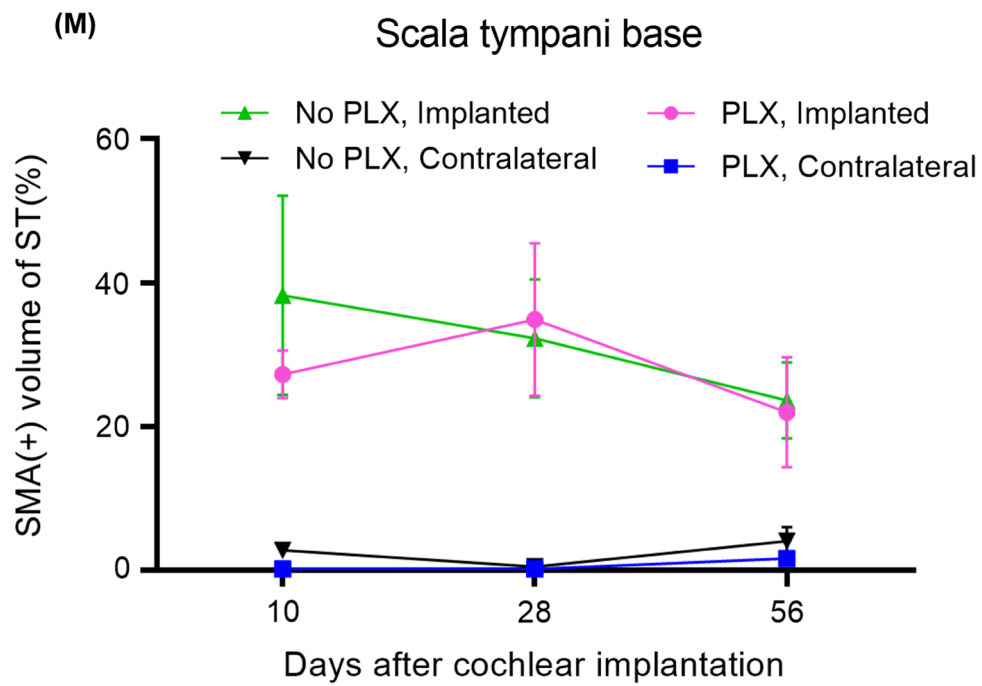
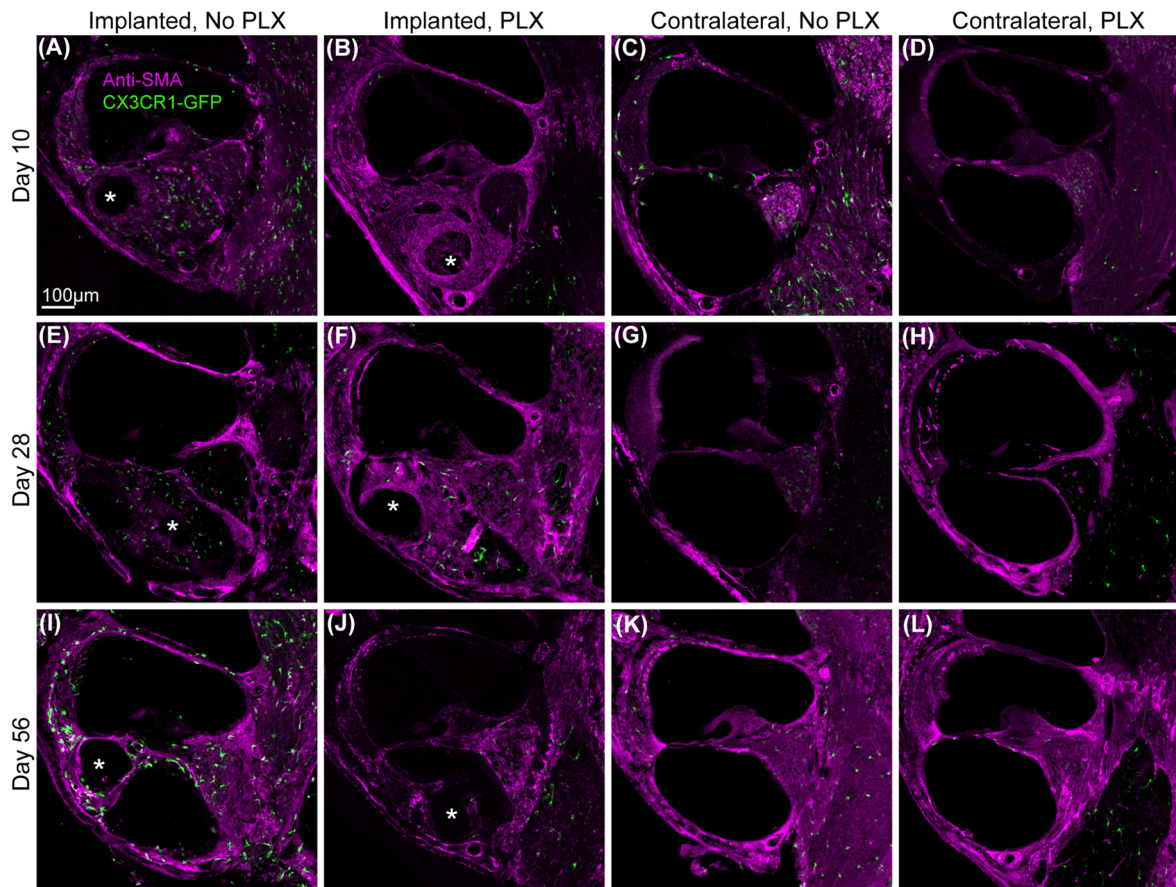


Fig. 5 (See legend on previous page.)

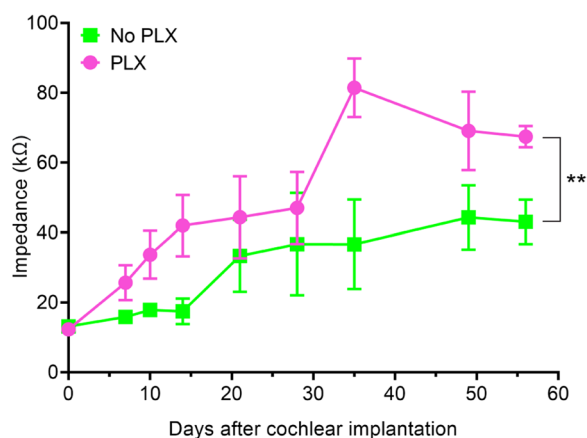


Fig. 6 Electrode impedance following cochlear implantation plotted over time. Lines represent mean impedance values across all functional electrodes (without open circuit) at the representative time points for the No PLX (green line) and PLX groups (pink line). Error bars indicate SEM. ** indicates $p < 0.001$

Discussion

Our data suggest that PLX5622, a specific inhibitor of CSF1R, at a dose of 1200 mg/kg for 7 days eliminated almost all cochlear mononuclear phagocytes. Following cochlear implantation, a cellular infiltration, including macrophages, with fibrotic tissue deposition occurs adjacent to the electrode array in the basal scala tympani and was associated with increased electrode impedance. When cochlear implantation was performed in mice with ongoing PLX 5622 macrophage depletion, cellular infiltration (including macrophage infiltration) was inhibited but the volume of fibrotic response was not. Electrical impedance following cochlear implantation trended higher in the PLX5622-treated group. Moreover, PLX5622 treatment was associated with the degeneration of SGNs in the base of the cochlea independent of cochlear implantation.

With short-term (7 days) administration of PLX5622 at a dose of 1200 mg/kg for 7 days, most CX3CR1-positive cells can be depleted from the cochlea. This dosage is also sufficient to deplete the brain microglia population [9]. It has been shown previously that CSF1R inhibition

by PLX5622 is not microglia-specific; it can affect other mononuclear phagocyte populations (monocyte, macrophage, and dendritic cells) as well [24]. Although there is preliminary evidence of a cochlear microglia population, their relative abundance compared to other mononuclear phagocytes like macrophages and dendritic cells has not been established [41]. CX3CR1 is expressed in all types of mononuclear phagocytes [12, 22, 53]. Here we observed that most, but not all, cochlear CX3CR1+ cells were depleted with short (or even long-term) treatment with PLX5622, suggesting differing susceptibility among mononuclear phagocytes. The relative susceptibility of individual types of mononuclear phagocytes to CSF1R inhibition by PLX5622 is yet to be determined as are dose-specific effects. Our data also support the previously published literature showing that sustained treatment with PLX5622 in CX3CR1^{GFP/+} mice results in a significant elimination of resident macrophages (~ 94%) without causing elevation of the ABR threshold. This study also suggests that CSF1R is expressed on the cochlear CX3CR1+ cells explaining the depletion of CX3CR1+ cells with CSF1R inhibitor PLX5622.

PLX5622 not only depleted resident CX3CR1+ cells before cochlear implantation, but it also caused sustained depletion of the infiltrating CX3CR1+ cells after placement of the electrode array. In this study, we have cautiously used the definition of ‘tissue-resident macrophages’ as a group of macrophages present in non-traumatized, uninfamed cochlear tissue from young mice. In our case, ‘cochlear tissue-resident macrophages’ represented by CX3CR1+ macrophages in a young mouse cochlea that has not been implanted. We determined whether PLX5622 can deplete ‘cochlear tissue-resident macrophages’ by treating unimplanted, CX3CR1^{+/-GFP} reporter mice with PLX5622 (PLX) and comparing them with age-matched, unimplanted CX3CR1^{+/-GFP} reporter mice.

On the other hand, we have defined ‘infiltrating/inflammatory macrophages’ as macrophages that infiltrate following a traumatic/inflammatory event (in our case, cochlear implantation). Infiltrating/inflammatory macrophages are thought to be derived from circulating

(See figure on next page.)

Fig. 7 Quantification of spiral ganglion neuron density following cochlear implantation. 7-day feeding on chow with 1200 ppm of PLX-5622 (PLX) or control chow (No PLX) was followed by cochlear implantation in CX3CR1^{+/-GFP} Thy1^{+/-YFP} mice. After recovery from surgical anesthesia, respective diets were resumed. Electrical stimulation was done as described before. Cochlea harvested at desired endpoints (10, 28, or 56 days) were sectioned at 30 μm thickness. **A–D** Representative images from the base of the cochlea. Quantification is shown for **E** base, **F** middle, **G** apex, **H** overall. After measurement of spiral ganglia volume and quantification of spiral ganglion neurons, SGN density was calculated by dividing the SGN count by the volume and expressed as per 10⁵ μm³. Density in 3 sections per animal was averaged. The number of the animals is considered the ‘n’ for this experiment. Number of cochlea used in this study are as follows: at day 10 post-CI, implanted ‘no PLX’ (n=4), implanted PLX, (n=3), contralateral ‘no PLX’ (n=3), contralateral PLX (n=5); at day 28 post-CI, implanted ‘no PLX’ (n=6), implanted PLX, (n=5), contralateral ‘no PLX’ (n=3), contralateral PLX (n=4); at day 56 post-CI, implanted ‘no PLX’ (n=3), implanted PLX, (n=6), contralateral ‘no PLX’ (n=3), contralateral PLX (n=4). Error bars indicate SEM. * indicates $p < 0.05$

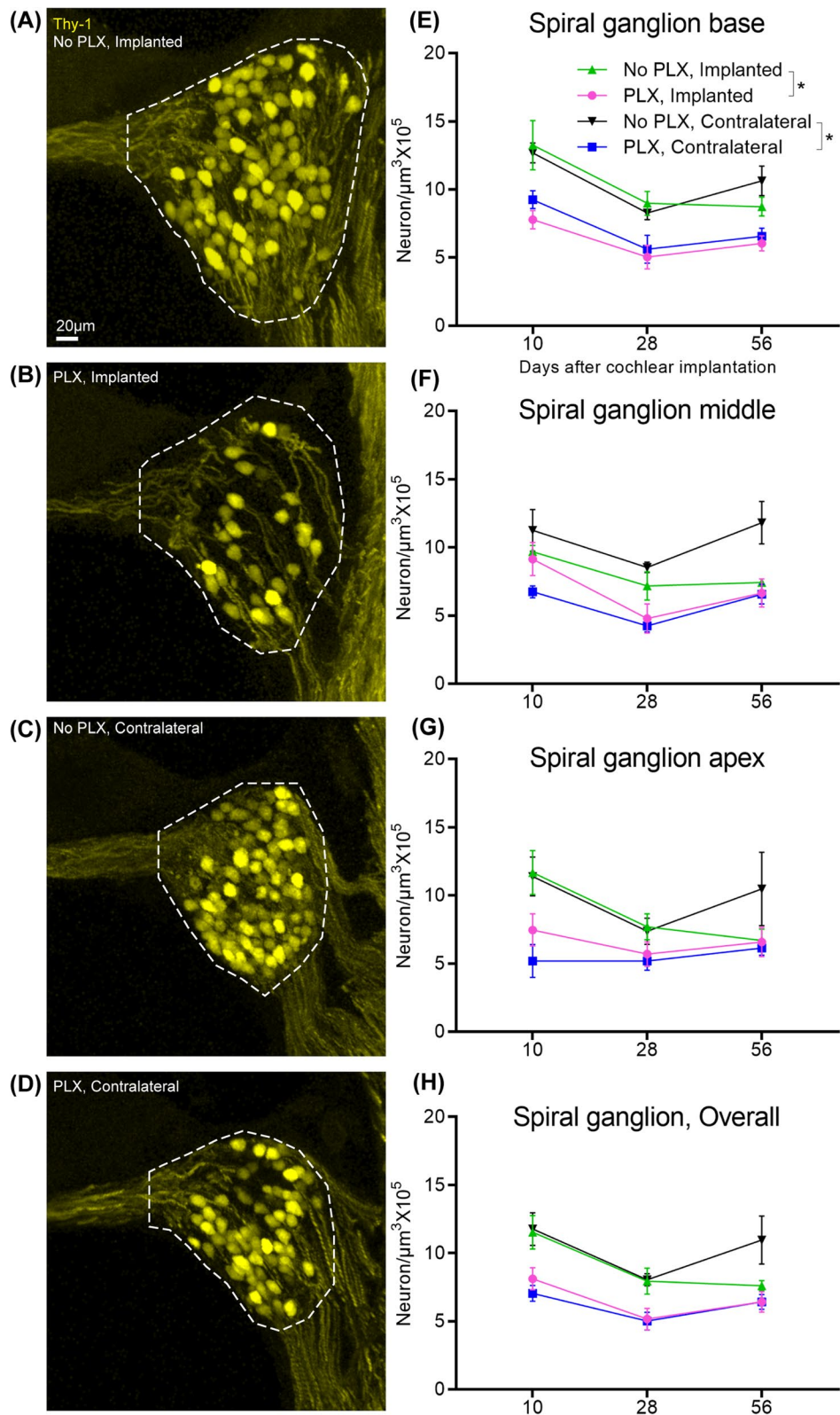


Fig. 7 (See legend on previous page.)

monocytes. To determine whether cochlear implantation can deplete infiltrating macrophages, we first depleted 'cochlear tissue-resident macrophages' with 7 days of treatment of PLX5622. Then, we implanted the cochlea where 'cochlear tissue-resident macrophages' were depleted. After implantation in these 'cochlear tissue-resident macrophage' free cochlea, we continued to treat these mice with PLX5622. This treatment effectively tests whether PLX5622 can deplete the infiltration of CX3CR1 + macrophages following cochlear implantation.

To the best of our knowledge, this is the first study to explore the role of CSF1R inhibition in a cochlear implant model. Studies on brain implants demonstrated similar effects on the brain microglial population [43]. They have shown that although PLX5622 treatment depletes microglia from the rat brain, astrocytes encapsulate the neuro-implant suggesting that microglia are redundant for this FBR in the brain. The reduction in cellular density in the scala tympani of PLX-treated mice following CI might be a direct effect of the elimination of resident and infiltrating macrophage population. Also, in the spiral ganglia, we observed degeneration of SGNs that can contribute to the decline in cellular density within the spiral ganglia. Moreover, macrophages also secrete growth and angiogenic factors [2].

Thus, the elimination of macrophages could indirectly reduce cellularity by decreasing cell proliferation and angiogenesis. Although macrophages are widely viewed as master regulators of the FBR to biomaterials, other innate and adaptive immune cells including T and B lymphocytes and mast cells contribute to these tissue responses [2]. In the cochlea, the FBR to the implanted electrode array occurs in a unique environment in the scala tympani that is otherwise devoid of cells. While the role of these other immune cells has not been studied intensively in the cochlea, it has been documented that T and B lymphocytes infiltrate the cochlea following cochlear implantation [30]. A wide range of cytokines can be secreted by activated macrophages; these include Interleukins (e.g., IL-1, IL-4, IL-5, IL-6, IL-8, IL-10, IL-12, IL-18), TNF- α , and TGF- β [2]. Many of these cytokines act as chemotactic factors for other immune cells. It is possible that depletion of resident and infiltrating macrophages by PLX5622 impacts recruitment of other immune cells and thus overall cellular infiltration of the scala tympani following CI.

One significant finding of these experiments is that the fibrotic response, as measured by anti- α -SMA immunolabeling, was not significantly reduced by PLX5622 treatment. These results mirror other studies that explored the role of CSF1R inhibition with PLX5622 on the FBR to neuro-implants in the brain. Sharon et al. showed that PLX5622 depletes microglia in rat brains [43], however,

it does not inhibit the astrocyte response encapsulating the neural implant [43]. These results with cochlear and neural implants are in sharp contrast with findings in non-neural tissue following the implantation of biomaterials. Doloff et al. demonstrated that following the implantation of biomaterials in non-neural tissue, the elimination of macrophages with CSF1R inhibitor effectively suppressed the fibrotic response. There are several plausible explanations for this difference between cochlear implantation and implantation in the peritoneal cavity performed by Doloff et al. including: 1. the likelihood that the pathophysiology of the FBR in neural tissue differs from that in non-neural tissue. Moreover, the peritoneal cavity provides a unique immunological niche that harbors specialized leukocyte populations supported by fat-associated lymphoid clusters (FALCs). On the other hand, among the neuronal tissues, the cochlea has a specialized immune environment where immune cells and non-immune, resident cells of cochlea, play immune functions [15]. Therefore, the comparison between implantation in the cochlea and peritoneal cavity appears to be a comparison between two specialized immunological niches. 2. The implanted biomaterials were different in cases of implantation in non-neural (peritoneal) tissue and elicited different, material-specific types of FBR. 3. The pharmacological agents that were used to deplete macrophages are different from what has been used in the neural tissue and had a different impact on fibrotic response. 4. Finally, cochlear implants were electrically stimulated, whereas the tissues implanted in Doloff et al. were not electrically stimulated. We have recognized an important limitation of our study: we used only one relatively specific marker (α -SMA) for quantification of the fibrotic response. However, the sensitivity of α -SMA as a marker for cochlear fibrotic response is not known. In our study, the depletion of CX3CR1 + cells with PLX5622 resulted in no change in α -SMA + fibrotic response. However, there are other markers of fibrotic response. While both α -SMA and collagen type 1A have been used as markers for post-CI fibrosis by Bas et al., the relative sensitivity of α -SMA as a marker of post-CI fibrotic response has never been examined [4]. This area needs to be further investigated. Using Col-EGFP/ α -SMA-RFP dual reporter mice, Sun et al. showed that only a minority of collagen-producing cells co-express α -SMA in the fibrotic lung and kidney suggesting that α -SMA may not be a sensitive marker of fibrotic response in those organs. Therefore, our study does not necessarily exclude changes in other molecular markers of fibrosis following cochlear implantation.

Following CI, there is a gradual rise in electrode impedances consistent with an evolving tissue response. PLX 5622 treatment leads to a more rapid rise in electrical

impedance compared to No PLX. As PLX5622 treatment reduces cellular infiltration into the cochlea, it appears that reducing cellular infiltration alone is not sufficient to prevent the rise in electrical impedance associated with the FBR. Further, the extent of fibrosis, as measured by anti- α -SMA immunolabeling, is not affected by PLX5622 treatment suggesting that the fibrotic tissue might be the factor maintaining the high electrical impedance in PLX5622 treated implanted cochlea. Moreover, electrode impedances in mice treated with PLX5622 rose more rapidly than the impedances in control mice raising the possibility that there are functional differences in the nature of the fibrotic response in the absence of macrophages. Post-implantation cochlear fibrosis is often accompanied by neo-ossification in humans and mice. The current study methods employed decalcification for histological preparation, prohibiting assessments of cochlear neo-ossification after implantation. This aspect is important for future studies, as CSF1R inhibition is associated with alterations in osteoclast activity that could impact post-CI neo-ossification and differentially affect electrode impedance compared to the less dense, non-mineralized fibrotic tissue [5].

Degeneration of SGNs in the base of the cochlea with PLX5622 treatment is noteworthy. The role of cochlear macrophages in the protection of SGNs depends on the model of cochlear insult. In a mouse model of selective hair cell destruction, fractalkine-mediated infiltration of CX3CR1 + mononuclear cells protect SGNs from degeneration [20]. Conversely, anti-inflammatory therapy with ibuprofen or dexamethasone has been shown to suppress the infiltration of macrophages in the spiral ganglion following aminoglycoside-induced hair cell loss in a rat model; this suppression of macrophage infiltration is associated with SGN protection [38].

Macrophage infiltration can be associated with the protection or degeneration of SGNs depending on context and chemokine receptor expression. CX3CR1 receptor deletion (CX3CR1KO) induces a distinct phenotype when compared to the depletion of CX3CR1 expressing cells, as we demonstrate here with PLX5622. One potential explanation is that macrophages play diverse roles in SGN protection in deafening models: the fractalkine pathway is involved in SGN protection, whereas macrophages are involved in additional mechanisms that contribute to SGN degeneration. Therefore, selective inhibition of fractalkine is neurotoxic whereas non-selective inhibition of inflammation provides neuroprotection following deafening. In a noise-induced cochlear synaptopathy model, macrophages promote synapse regeneration [26].

In the present study, macrophage infiltration into the spiral ganglia following cochlear implantation itself does

not appear to cause SGN degeneration. We observed SGN degeneration in the base of the cochlea following PLX5622 treatment independent of cochlear implant surgery. This observation suggests a general protective role of macrophages for SGNs. Bas et al. have shown that 7 days after cochlear implantation in a murine model, arginase 1 (Arg1) positive, M2 macrophages infiltrate into the cochlea, primarily into the spiral ganglion [4].

M2 macrophages are thought to engulf and digest dead cells, debris, and extracellular matrix components that promote activation of tissue-damaging M1 macrophages [28]. M2 macrophages are also believed to secrete immunoregulatory cytokines (e.g., IL-10) and activate immunoregulatory T lymphocytes (T_{reg}) [28]. A potential explanation for SGN degeneration following the depletion of macrophages with PLX5622 is that it depletes the neuroprotective, anti-inflammatory M2 macrophages within the spiral ganglion.

However, there is an important confounder that makes the interpretation of our data more complex. Our experiments were done on mice with a C57BL/6J/B6 background, whereas other deafening and synaptopathy experiments were performed on CBA/J mice and rats. C57BL/6J/B6 mice exhibit early onset hearing loss and SGN loss that is not observed in CBA/J mice or rats [19]. Importantly, the C57BL/6J/B6 background mimics hearing loss patterns seen in many human CI candidates with the post-lingual onset of high-frequency hearing loss [17]. One plausible explanation for our results is that macrophages play a protective role for SGNs in C57BL/6J/B6 mice and in the absence of macrophages, early onset SGN degeneration is accelerated. Experiments inhibiting CSF1R with PLX5622 in mice with CBA/J backgrounds can provide additional insights into this issue.

We would like to mention a potential limitation of the method of SGN quantification that we used. We observed variation in Thy1-driven YFP expression among the SGN population. Therefore, the use of Thy1-reporter expression as a marker for SGN might present issues with reliability. Moreover, the sensitivity of Thy1-reporter as a marker for SGN is not currently known. These present findings are relevant to current efforts to develop pharmacologic-based therapies to mitigate the effects of CI insertion trauma, as the effect of dexamethasone eluting electrode arrays (NCT04750642, NCT04450290) on macrophage suppression and subsequent SGN preservation or degeneration is not yet clear. In a human study, post-CI inflammatory foreign body response has been shown to be associated with degeneration of SGNs [29]. Data from guinea pig model of cochlear implantation suggested that a healthy SGN population is required for optimum neural response to electrical stimulation [36, 40]. Elucidating the impact of macrophages on post-CI

SGN health is relevant for the development of more targeted strategies for selectively mitigating maladaptive aspects of the inflammatory response. As corticosteroids are nonspecific immunosuppressive agents, they might exert unwanted side effects and a more specific immunosuppressive agent might be more beneficial in this context.

In summary, our study suggests that macrophages (mononuclear phagocytes) play an important role in the intracochlear tissue remodeling that occurs following CI and in SGN health. Depletion of macrophages with PLX5622 reduces cellular infiltration into the scala media, but not fibrosis, following cochlear implantation. Moreover, macrophages appear to modulate the dynamics of fibrosis contributing to increases in electrode impedances. Depleting a specific subset of mononuclear phagocytes (e.g., dendritic cells), lymphocytes, or non-immune cells will provide valuable information about their role in the post-CI FBR and inform translational efforts to mitigate this response. The current study describes the unique role of macrophages in cellular infiltration, fibrosis, and SGN health following implantation. Further work is needed to understand the interplay of other immunologic cells following cochlear implantation that, along with macrophages, contribute to post-CI cochlear inflammation and FBR.

Abbreviations

CI	Cochlear implant
FBR	Foreign body response
SGN	Spiral ganglion neuron
ECAP	Electrically evoked compound action
CSF-1	Colony stimulating factor-1
PCR	Polymerase chain reaction
DNA	Deoxyribonucleic acid
CL	Current level
PBS	Phosphate buffer solution
PFA	Paraformaldehyde

Acknowledgements

We thank Dr. Shakila Mahmuda Fatima for generous help in reviewing and formatting the manuscript.

Author contributions

MRH, KH, MTR, JRK, and ADC: conceived of the presented idea. MTR, BJM, BH, US, PE, and IR: carried out the experiments. MTR, BH, US, ADC, IR, FN, NAK, PE, SC, JO, MRH: analyzed the data. IR prepared figures with support from MTR, MRH, and ADC. MTR wrote the manuscript with support from MRH, ADC, KH, JRK, BJM, IR, JO, and SC. All authors reviewed the manuscript.

Funding

National Institute on Deafness and Other Communication Disorders, F32DC020643. National Institute on Deafness and Other Communication Disorders, R01DC018488. National Institute on Deafness and Other Communication Disorders, R01DC012578. National Institute on Deafness and Other Communication Disorders, P50 DC00242. National Institute on Deafness and Other Communication Disorders, U54TR001013.

Availability of data and materials

Data supporting and validating the findings of this study are available within this article and its supplementary materials.

Declarations

Ethics approval and consent to participate

Protocols for the use of animals in all experiments in this study were approved by the University of Iowa's Institutional Animal Care and Use Committee (IACUC), consistent with the Guide for the Care and Use of Laboratory Animals from Institute for Laboratory Animal Research, National Research Council. No human subjects were involved and therefore consent to participate is not applicable.

Consent for publication

Not applicable.

Competing interests

Marlan R. Hansen is a co-founder and Chief Medical Officer of IotaMotion Inc. and a co-founder of ZwiCoat Materials Innovations, Inc with equity interest.

Author details

¹Department of Otolaryngology-Head and Neck Surgery, The University of Iowa, Iowa City, IA 52242, USA. ²Department of Biostatistics, The University of Iowa, Iowa City, IA, USA. ³Cochlear Limited, Sydney, Australia. ⁴Department of Otolaryngology-Head and Neck Surgery, Washington University School of Medicine, St. Louis, MO, USA.

Received: 12 June 2023 Accepted: 10 November 2023

Published online: 16 November 2023

References

- Ahmadi N, Gausterer JC, Honeder C, Motz M, Schopper H, Zhu C, et al. Long-term effects and potential limits of intratympanic dexamethasone-loaded hydrogels combined with dexamethasone-eluting cochlear electrodes in a low-insertion trauma Guinea pig model. *Hear Res.* 2019;384:107825. <https://doi.org/10.1016/j.heares.2019.107825>.
- Anderson JM, Rodriguez A, Chang DT. Foreign body reaction to biomaterials. *Semin Immunol.* 2008;20(2):86–100. <https://doi.org/10.1016/j.smim.2007.11.004>.
- Bas E, Bohorquez J, Goncalves S, Perez E, Dinh CT, Garnham C, Van De Water TR, et al. Electrode array-eluted dexamethasone protects against electrode insertion trauma induced hearing and hair cell losses, damage to neural elements, increases in impedance and fibrosis: a dose response study. *Hear Res.* 2016;337:12–24. <https://doi.org/10.1016/j.heares.2016.02.003>.
- Bas E, Goncalves S, Adams M, Dinh CT, Bas JM, Van De Water TR, Eshraghi AA. Spiral ganglion cells and macrophages initiate neuro-inflammation and scarring following cochlear implantation. *Front Cell Neurosci.* 2015;9:303. <https://doi.org/10.3389/fncel.2015.00303>.
- Brun J, Andreasen CM, Ejersted T, Andersen TL, Caverzasio J, Thouverey C. PDGF receptor signaling in osteoblast lineage cells controls bone resorption through upregulation of Csf1 expression. *J Bone Miner Res.* 2020;35(12):2458–69. <https://doi.org/10.1002/jbmr.4150>.
- Clark GM, Shute SA, Shepherd RK, Carter TD. Cochlear implantation: osteoneogenesis, electrode-tissue impedance, and residual hearing. *Ann Otol Rhinol Laryngol Suppl.* 1995;166:40–2.
- Claussen AD, Quevedo RV, Kirk JR, Higgins T, Mostaert B, Rahman MT, Hansen MR, et al. Chronic cochlear implantation with and without electric stimulation in a mouse model induces robust cochlear influx of CX3CR1(+)/GFP macrophages. *Hear Res.* 2022;426:108510. <https://doi.org/10.1016/j.heares.2022.108510>.
- Claussen AD, Vielman Quevedo R, Mostaert B, Kirk JR, Dueck WF, Hansen MR. A mouse model of cochlear implantation with chronic electric stimulation. *PLoS ONE.* 2019;14(4):e0215407. <https://doi.org/10.1371/journal.pone.0215407>.
- Dagher NN, Najafi AR, Kayala KM, Elmore MR, White TE, Medeiros R, Green KN, et al. Colony-stimulating factor 1 receptor inhibition prevents microglial plaque association and improves cognition in 3xTg-AD mice. *J Neuroinflammation.* 2015;12:139. <https://doi.org/10.1186/s12974-015-0366-9>.
- Davies LC, Jenkins SJ, Allen JE, Taylor PR. Tissue-resident macrophages. *Nat Immunol.* 2013;14(10):986–95. <https://doi.org/10.1038/ni.2705>.

11. Feng G, Mellor RH, Bernstein M, Keller-Peck C, Nguyen QT, Wallace M, Nerbonne JM, Lichtman JW, Sanes JR. Imaging neuronal subsets in transgenic mice expressing multiple spectral variants of GFP. *Neuron*. 2000;28(1):41–51. [https://doi.org/10.1016/s0896-6273\(00\)00084-2](https://doi.org/10.1016/s0896-6273(00)00084-2).
12. Feng J, Pucella JN, Jang G, Alcantara-Hernandez M, Upadhaya S, Adams NM, Reizis B, et al. Clonal lineage tracing reveals shared origin of conventional and plasmacytoid dendritic cells. *Immunity*. 2022;55(3):405–22. <https://doi.org/10.1016/j.immuni.2022.01.016>.
13. Foggia MJ, Quevedo RV, Hansen MR. Intracochlear fibrosis and the foreign body response to cochlear implant biomaterials. *Laryngoscope Investig Otolaryngol*. 2019;4(6):678–83. <https://doi.org/10.1002/liv.2.329>.
14. Hoeffel G, Ginhoux F. Ontogeny of tissue-resident macrophages. *Front Immunol*. 2015;6:486. <https://doi.org/10.3389/fimmu.2015.00486>.
15. Hu BH, Zhang C, Frye MD. Immune cells and non-immune cells with immune function in mammalian cochlea. *Hear Res*. 2018;362:14–24. <https://doi.org/10.1016/j.heares.2017.12.009>.
16. Ishiyama A, Ishiyama G, Lopez IA, Linthicum FH Jr. Temporal bone histopathology of first-generation cochlear implant electrode translocation. *Otol Neurotol*. 2019;40(6):e581–91. <https://doi.org/10.1097/MAO.000000000000247>.
17. Jensen MJ, Claussen AD, Higgins T, Vielman-Quevedo R, Mostaert B, Xu L, Kirk J, Hansen MR. Cochlear implant material effects on inflammatory cell function and foreign body response. *Hear Res*. 2022;426:108597. <https://doi.org/10.1016/j.heares.2022.108597>.
18. Jung S, Aliberti J, Graemmel P, Sunshine MJ, Kreutzberg GW, Sher A, Littman DR. Analysis of fractalkine receptor CX(3)CR1 function by targeted deletion and green fluorescent protein reporter gene insertion. *Mol Cell Biol*. 2000;20(11):4106–14. <https://doi.org/10.1128/MCB.20.11.4106-4114.2000>.
19. Kane KL, Longo-Guess CM, Gagnon LH, Ding D, Salvi RJ, Johnson KR. Genetic background effects on age-related hearing loss associated with Cdh23 variants in mice. *Hear Res*. 2012;283(1–2):80–88. <https://doi.org/10.1016/j.heares.2011.11.007>.
20. Kaur T, Zamani D, Tong L, Rubel EW, Ohlemiller KK, Hirose K, Warchol ME. Fractalkine signaling regulates macrophage recruitment into the cochlea and promotes the survival of spiral ganglion neurons after selective hair cell lesion. *J Neurosci*. 2015;35(45):15050–61. <https://doi.org/10.1523/JNEUROSCI.2325-15.2015>.
21. Kopelovich JC, Cagaanan AP, Miller CA, Abbas PJ, Green SH. Intracochlear electrical stimulation suppresses apoptotic signaling in rat spiral ganglion neurons after deafening in vivo. *Otolaryngol Head Neck Surg*. 2013;149(5):745–52. <https://doi.org/10.1177/0194599813498702>.
22. Kosco B, Kurapati S, Rodrigues RR, Nedjic J, Gowda K, Shin C, Bogunovic M, et al. Gut-resident CX3CR1(hi) macrophages induce tertiary lymphoid structures and IgA response in situ. *Sci Immunol*. 2020. <https://doi.org/10.1126/sciimmunol.aax0062>.
23. Lavin Y, Merad M. Macrophages: gatekeepers of tissue integrity. *Cancer Immunol Res*. 2013;1(4):201–9. <https://doi.org/10.1158/2326-6066.CIR-13-0117>.
24. Lei F, Cui N, Zhou C, Chodosh J, Vavvas DG, Paschalis EI. CSF1R inhibition by a small-molecule inhibitor is not microglia specific; affecting hematopoiesis and the function of macrophages. *Proc Natl Acad Sci U S A*. 2020;117(38):23336–23338. <https://doi.org/10.1073/pnas.1922788117>.
25. Liu Y, Jolly C, Braun S, Janssen T, Scherer E, Steinhoff J, Kiefer J, et al. Effects of a dexamethasone-releasing implant on cochleae: a functional, morphological and pharmacokinetic study. *Hear Res*. 2015;327:89–101. <https://doi.org/10.1016/j.heares.2015.04.019>.
26. Manickam V, Gawande DY, Stothert AR, Clayman AC, Batalina L, Warchol ME, Kaur T, et al. Macrophages promote repair of inner hair cell ribbon synapses following noise-induced cochlear synaptopathy. *J Neurosci*. 2023;43(12):2075–89. <https://doi.org/10.1523/JNEUROSCI.1273-22.2023>.
27. Manrique-Huarte R, Zulueta-Santos C, Calavia D, Linera-Alperi MA, Gallego MA, Jolly C, Manrique M. Cochlear implantation with a dexamethasone eluting electrode array: functional and anatomical changes in non-human primates. *Otol Neurotol*. 2020;41(7):e812–22. <https://doi.org/10.1097/MAO.0000000000002686>.
28. Murray PJ, Wynn TA. Protective and pathogenic functions of macrophage subsets. *Nat Rev Immunol*. 2011;11(11):723–37. <https://doi.org/10.1038/nri3073>.
29. Nadol JB Jr, Eddington DK, Burgess BJ. Foreign body or hypersensitivity granuloma of the inner ear after cochlear implantation: one possible cause of a soft failure? *Otol Neurotol*. 2008;29(8):1076–84. <https://doi.org/10.1097/MAO.0b013e31818c33cf>.
30. Nadol JB Jr, O'Malley JT, Burgess BJ, Galler D. Cellular immunologic responses to cochlear implantation in the human. *Hear Res*. 2014;318:11–7. <https://doi.org/10.1016/j.heares.2014.09.007>.
31. Ni D, Shepherd RK, Seldon HL, Xu SA, Clark GM, Millard RE. Cochlear pathology following chronic electrical stimulation of the auditory nerve. I: normal hearing kittens. *Hear Res*. 1992;62(1):63–81. [https://doi.org/10.1016/0378-5955\(92\)90203-y](https://doi.org/10.1016/0378-5955(92)90203-y).
32. Noonan KY, Lopez IA, Ishiyama G, Ishiyama A. Immune response of macrophage population to cochlear implantation: cochlea immune cells. *Otol Neurotol*. 2020;41(9):1288–95. <https://doi.org/10.1097/MAO.0000000000002764>.
33. O'Leary SJ, Monksfield P, Kel G, Connolly T, Souter MA, Chang A, Eastwood H, et al. Relations between cochlear histopathology and hearing loss in experimental cochlear implantation. *Hear Res*. 2013;298:27–35. <https://doi.org/10.1016/j.heares.2013.01.012>.
34. O'Malley JT, Nadol JB Jr, McKenna MJ. Anti CD163+, Iba1+, and CD68+ cells in the adult human inner ear: normal distribution of an unappreciated class of macrophages/microglia and implications for inflammatory otopathology in humans. *Otol Neurotol*. 2016;37(1):99–108. <https://doi.org/10.1097/MAO.0000000000000879>.
35. Okayasu T, Quesnel AM, O'Malley JT, Kamakura T, Nadol JB Jr. The distribution and prevalence of macrophages in the cochlea following cochlear implantation in the human: an immunohistochemical study using anti-iba1 antibody. *Otol Neurotol*. 2020;41(3):e304–16. <https://doi.org/10.1097/MAO.0000000000002495>.
36. Pflugst BE, Hughes AP, Colesa DJ, Watts MM, Strahl SB, Raphael Y. Insertion trauma and recovery of function after cochlear implantation: evidence from objective functional measures. *Hear Res*. 2015;330(Pt A):98–105. <https://doi.org/10.1016/j.heares.2015.07.010>.
37. Quesnel AM, Nakajima HH, Rosowski JJ, Hansen MR, Gantz BJ, Nadol JB Jr. Delayed loss of hearing after hearing preservation cochlear implantation: human temporal bone pathology and implications for etiology. *Hear Res*. 2016;333:225–34. <https://doi.org/10.1016/j.heares.2015.08.018>.
38. Rahman MT, Chari DA, Ishiyama G, Lopez I, Quesnel AM, Ishiyama A, Hansen MR, et al. Cochlear implants: causes, effects and mitigation strategies for the foreign body response and inflammation. *Hear Res*. 2022;422: 108536. <https://doi.org/10.1016/j.heares.2022.108536>.
39. Roche JP, Hansen MR. On the horizon: cochlear implant technology. *Otolaryngol Clin North Am*. 2015;48(6):1097–116. <https://doi.org/10.1016/j.otc.2015.07.009>.
40. Schwartz-Leyzac KC, Colesa DJ, Buswinka CJ, Rabah AM, Swiderski DL, Raphael Y, Pflugst BE. How electrically evoked compound action potentials in chronically implanted guinea pigs relate to auditory nerve health and electrode impedance. *J Acoust Soc Am*. 2020;148(6):3900. <https://doi.org/10.1121/1.5000288>.
41. Seigel GM, Manohar S, Bai YY, Ding D, Salvi R. An immortalized microglial cell line (Mocha) derived from rat cochlea. *Mol Cell Neurosci*. 2017;85:202–10. <https://doi.org/10.1016/j.mcn.2017.11.001>.
42. Seyyedi M, Nadol JB Jr. Intracochlear inflammatory response to cochlear implant electrodes in humans. *Otol Neurotol*. 2014;35(9):1545–51. <https://doi.org/10.1097/MAO.0000000000000540>.
43. Sharon A, Jankowski MM, Shmoel N, Erez H, Spira ME. Inflammatory foreign body response induced by neuro-implants in rat cortices depleted of resident microglia by a CSF1R inhibitor and its implications. *Front Neurosci*. 2021;15: 646914. <https://doi.org/10.3389/fnins.2021.646914>.
44. Shaul C, Bester CW, Weder S, Choi J, Eastwood H, Padmavathi KV, O'Leary SJ, et al. Electrical impedance as a biomarker for inner ear pathology following lateral wall and peri-modiolar cochlear implantation. *Otol Neurotol*. 2019;40(5):e518–26. <https://doi.org/10.1097/MAO.0000000000000227>.
45. Shepherd RK, Clark GM, Xu SA, Pyman BC. Cochlear pathology following reimplantation of a multichannel scala tympani electrode array in the macaque. *Am J Otol*. 1995;16(2):186–99.
46. Shepherd RK, Matsushima J, Millard RE, Clark GM. Cochlear pathology following chronic electrical stimulation using non charge balanced stimuli. *Acta Otolaryngol*. 1991;111(5):848–60. <https://doi.org/10.3109/00016489109138421>.

47. Simoni E, Gentilin E, Candito M, Borile G, Romanato F, Chicca M, Astolfi L, et al. Immune response after cochlear implantation. *Front Neurol*. 2020;11:341. <https://doi.org/10.3389/fneur.2020.00341>.
48. Spangenberg E, Severson PL, Hohsfield LA, Crapser J, Zhang J, Burton EA, Green KN, et al. Sustained microglial depletion with CSF1R inhibitor impairs parenchymal plaque development in an Alzheimer's disease model. *Nat Commun*. 2019;10(1):3758. <https://doi.org/10.1038/s41467-019-11674-z>.
49. Stanley ER, Chitu V. CSF-1 receptor signaling in myeloid cells. *Cold Spring Harb Perspect Biol*. 2014. <https://doi.org/10.1101/cshperspect.a021857>.
50. Tykocinski M, Cohen LT, Cowan RS. Measurement and analysis of access resistance and polarization impedance in cochlear implant recipients. *Otol Neurotol*. 2005;26(5):948–56. <https://doi.org/10.1097/01.mao.0000185056.99888.f3>.
51. Van De Water TR, Abi Hachem RN, Dinh CT, Bas E, Haake SM, Hoosien G, Balkany TJ, et al. Conservation of hearing and protection of auditory hair cells against trauma-induced losses by local dexamethasone therapy: molecular and genetic mechanisms. *Cochlear Implants Int*. 2010;11(Suppl 1):42–55. <https://doi.org/10.1179/146701010X12671178390834>.
52. Wilk M, Hessler R, Mugridge K, Jolly C, Fehr M, Lenarz T, Scheper V. Impedance changes and fibrous tissue growth after cochlear implantation are correlated and can be reduced using a dexamethasone eluting electrode. *PLoS ONE*. 2016;11(2): e0147552. <https://doi.org/10.1371/journal.pone.0147552>.
53. Wolf Y, Yona S, Kim KW, Jung S. Microglia, seen from the CX3CR1 angle. *Front Cell Neurosci*. 2013;7:26. <https://doi.org/10.3389/fncel.2013.00026>.
54. Xu J, Shepherd RK, Millard RE, Clark GM. Chronic electrical stimulation of the auditory nerve at high stimulus rates: a physiological and histopathological study. *Hear Res*. 1997;105(1–2):1–29. [https://doi.org/10.1016/s0378-5955\(96\)00193-1](https://doi.org/10.1016/s0378-5955(96)00193-1).
55. Zhang H, Stark G, Reiss L. Changes in gene expression and hearing thresholds after cochlear implantation. *Otol Neurotol*. 2015;36(7):1157–65. <https://doi.org/10.1097/MAO.0000000000000787>.

Publisher's Note

Springer Nature remains neutral with regard to jurisdictional claims in published maps and institutional affiliations.

Ready to submit your research? Choose BMC and benefit from:

- fast, convenient online submission
- thorough peer review by experienced researchers in your field
- rapid publication on acceptance
- support for research data, including large and complex data types
- gold Open Access which fosters wider collaboration and increased citations
- maximum visibility for your research: over 100M website views per year

At BMC, research is always in progress.

Learn more biomedcentral.com/submissions

